EDN: IMICDE
УДК 538.9

Temperature Resistance of Silver and Iron Nanoparticles

Bair B. Damdinov*
Siberian Federal University
Krasnoyarsk, Russian Federation
Institute of Physical Materials Science SB RAS
Ulan-Ude, Russian Federation
Aleksandr A. Ershov
Chingis M. Mitypov
Siberian Federal University
Krasnoyarsk, Russian Federation
Olga A. Maximova
Siberian Federal University
Krasnoyarsk, Russian Federation
Kirensky Institute of Physics, Federal Research Center KSC SB RAS
Krasnoyarsk, Russian Federation
Galina N. Haruk
Siberian Federal University
Krasnoyarsk, Russian Federation

Received 12.01.2023, received in revised form 02.02.2024, accepted 14.03.2024

Abstract. In this work, a study of iron and silver nanoparticles was carried out by Raman spectroscopy. The spectra were obtained by changing the temperature. The positions of individual spectral lines were found to determine the presence or absence of second-order phase transitions. Based on the data on the shift of spectral lines, one can also draw a conclusion about the stability of the objects of study under changing external conditions and how this affects changes in the suspensions in which they are included. Absorption coefficients were measured, and the sizes of the studied nanoparticles in aqueous suspensions were determined.

Keywords: suspensions of iron and silver nanoparticles, lubricants, Raman scattering of light, shift of spectral lines.

Citation: B.B. Damdinov, A.A. Ershov, C.M. Mitypov, O.A. Maximova, G.N. Haruk, Temperature Resistance of Silver and Iron Nanoparticles, J. Sib. Fed. Univ. Math. Phys., 2024, 17(4), 497–505. EDN: IMICDE.

Interest in nanoparticles arose at the end of the last century and has been continuously growing since then. The area of application of nanoparticles is also expanding. For instance, they are used as catalysts for chemical reactions, and special coatings are created to absorb solar energy The efficiency of using nanoparticles depends on many factors, such as surface chemistry, size, size distribution, shape, particle morphology, particle composition, agglomeration and dissolution rate, reactivity of particles in solutions, etc. [1]. Nanoparticles of metals such as iron and silver have found great use in medicine. For example, the most famous property of iron nanoparticles (FeNPs) is that it can be used as a material that destroys the membrane of cancer cells, while silver nanoparticles (AgNPs) are used as a sterilizing material, which is best shown by drugs based on colloidal silver used as a biologically active additive [2–7]. In addition to medical applications, FeNPs and AgNPs are widely used in electronics and technological processes [2–4].

*dababa@mail.ru https://orcid.org/0000-0003-0914-0096

The increased interest is primarily associated with the manifestation of properties that are different from the properties of systems consisting of coarse particles. In particular, these special properties make the properties of suspensions, in which nanoparticles are an integral part, also non-standard. Suspensions of nanoparticles, also called nanofluids, have received a wide range of applications. At present, much attention is paid to the creation of highly efficient lubricants with improved properties through the use of ultrafine powders with particles 10–100 nm in size and a specific surface area up to 450 m^{-2}/g. The effectiveness of the use of nanomaterials and nanofunctional additives is confirmed by the results of studies [8–11]. For example, in [8], expressions were obtained for the dependence of the efficiency, power loss due to friction, taking into account the presence of nanoparticles in lubricants. The derivation of a relation describing the change in the viscosity of a lubricant composite material on the volume of a dispersed filler is presented. The study [9] proposed a new rheological model of suspensions based on the generalized Casson model and showed its application to particles of various shapes and sizes in media with different viscosities. The injection of nanosized SiO_2, FeO, Fe_2O_3, Na_2O, K_2O particles into the lubricating medium makes it possible to improve the antifriction and antiwear properties of tribocouplers of the support units of mechanisms and machines [12]. Nanotribological studies carried out by domestic and foreign researchers have shown that fullerenes and fullerene blacks can be successfully used as antifriction, antiwear, and antiseize additives [13,14]. In [15,16], the mechanical properties of thin lubricating layers of several molecular diameters of octamethylcyclotetrasiloxane were studied using a surface force apparatus, it was shown that the sliding of liquid layers is in good agreement with expectations based on bulk viscosity, while sliding in the upper part solid substrate is 35 times higher. Experimental studies of the rheological properties of lubricating oils with and without nanoparticles show that nanoparticles have a significant effect on rheological parameters [17]. The results showed that the apparent viscosity increases with increasing concentration of nanoparticles. In this regard, it seems relevant to study the viscoelastic properties of colloidal suspensions of nanoparticles by various methods.

Metal nanoparticles are used as materials that complement research methods, improving their qualitative and quantitative characteristics. They are used especially effectively to obtain giant Raman scattering, which makes it possible to obtain spectra of higher intensity compared to its traditional technique [18,19]. Since Raman spectroscopy is one of the most sensitive and powerful non-destructive optical spectral measurement methods, it was chosen as a method for studying FeNPs and AgNPs at various temperatures.

In this work, iron and silver nanoparticles were studied using Raman spectroscopy. It has been established that the position of individual spectral lines determines the presence or absence of second-order phase transitions. For the first time, the ultrasound attenuation spectra of suspensions were measured. The difference in the behaviour of the attenuation coefficient for AgNPs suspension and FeNPs suspension from the ultrasound frequency was shown.

1. Experiment

The measurements were carried out in order to determine the presence or absence of phase transitions, which may be evidenced by a significant shift in the spectral lines or a significant change in the spectral composition. The substances under study were iron [20] and silver [21] nanoparticles, since there are no data for them obtained by Raman spectroscopy at temperatures below room temperature [22,23]. The spectra of silver nanoparticles were obtained in the frequency range of 180–3200 cm^{-1}, and the spectra of iron nanoparticles in the range of 20–1200 cm^{-1}. Since FeNPs have a much higher absorption capacity compared to AgNPs, it took an order of magnitude longer time for signal accumulation to obtain spectra with resolvable lines

The spectra were obtained on a Horiba Jobin Yvon T64000 triple Raman spectrometer. The

excitation source was solid-state laser radiation at a wavelength of 532 nm. The spectral resolution at which the Raman spectra (RS) were obtained was 2 cm^{-1} for both FeNPs and AgNPs. The measurements were carried out with a temperature change in the range of 223–328 K, with a stabilization accuracy better than 0.1 K. All spectral data were obtained in backscattering geometry.

Particle suspensions with a mass concentration of 1% were prepared. Suspensions were prepared using a two-stage method. First, the particle powder was mixed in distilled water using a high-speed stirrer during 30 minutes, and after that it was treated with an ultrasound disperser UZTA-0.4/22-OM (power 400 W, frequency 22 kHz, 30 minutes).

Ultrasound attenuation spectra of 1 wt.% suspensions were measured using an acoustic and electroacoustic spectrometer DT1202 (Dispersion Technologies). In addition, this device allows you to determine the particle size distribution over a wide range of particle concentrations. The acoustic sensor of the device measures the attenuation coefficient of ultrasound in a wide dynamic frequency range (from 3 to 100 MHz). The spectrometer has a chamber in which an ultrasound wave emitter and an ultrasound signal receiver are located. The chamber is filled with the test liquid, in which ultrasound propagates from the emitter to the receiver. In this case, ultrasound waves are scattered by particles, which leads to changes in the spectrum of the ultrasound signal, which is recorded by the device.

2. Results and discussion

Let us consider AgNPs first. Since the spectra extend over a wide frequency range, to simplify their processing, the obtained spectra were divided into three frequency ranges: 180–950 cm^{-1}, 950–1770 cm^{-1} and 2780–3200 cm^{-1}. The frequency interval 1770–2780 cm^{-1} is not subject to investigation, since no spectral lines with the intensity exceeding the noise level were found in our spectra of this frequency range.

In the frequency range 180–950 cm^{-1} (Fig. 1), it is inappropriate to divide the experimental contour into components due to the proximity of overlapping low-intensity spectral lines, which makes it impossible to trace the positions of individual lines.

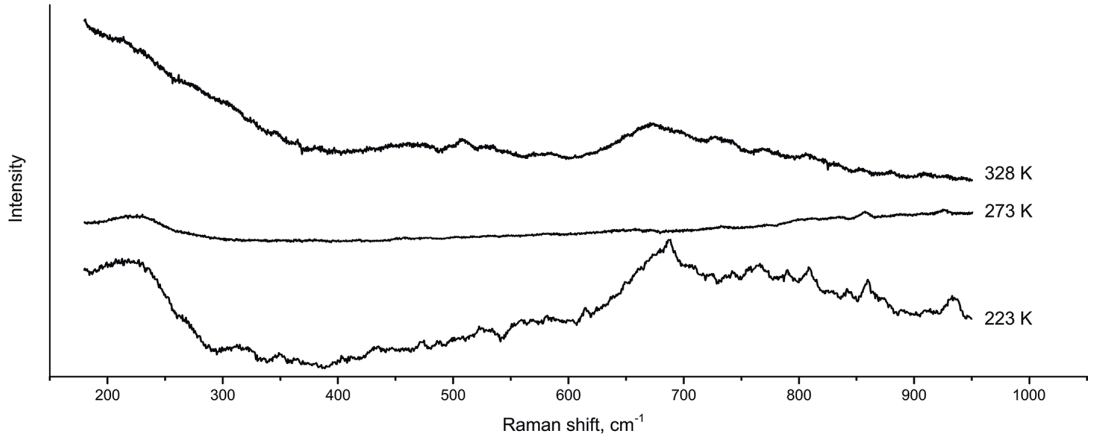

Fig. 1. Raman spectra of AgNPs at various temperatures (indicated to the right of the spectrum) in the frequency range 180–950 cm^{-1}

In Fig. 2a, the two most intense lines correspond to vibrations of the carbon atom, which is explained by the AgNPs synthesis method. Also, as a result of the interaction of Ag nanoparticles with air and carbon, a large number of additional spectral contours appear. Due to the strong

electrostatic interaction between the nanoparticles of the studied substance and the detected elements, the lines corresponding to Ag vibrations cannot be detected in their pure form.

In Fig. 2b, there are no sharp jumps in the intensities of individual lines; therefore, in the frequency range of 2780–3200 cm^{-1}, the most obvious pattern of line positions is presented.

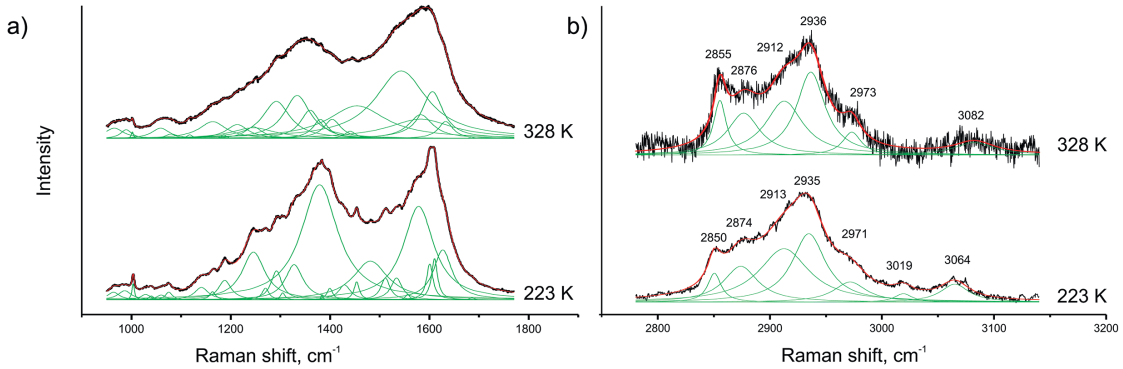

Fig. 2. Raman spectra of AgNPs at different temperatures (indicated to the right of the spectrum) divided into different ranges: a) 950–1770 cm^{-1}, b) 2780–3200 cm^{-1} (frequencies in cm^{-1} are indicated above the spectra)

In this regard, dependences of the position of the Raman lines on temperature were plotted (Fig. 3). It can be seen from the figure that the shifts of the lines are small and new lines do not appear. The disappearance of the line at a frequency of 3019 cm^{-1} at a temperature of 313 K occurs due to a decrease in its intensity, that is why the signal-to-noise ratio does not allow it to be further resolved. The highest frequency component of the spectrum undergoes the greatest shift. With an increase in temperature and a strong influence of noise, the determination of its position has an error of the order of 7 cm^{-1}. The high level of noise with respect to the signal is explained by the presence of chemisorption in the test substance [24].

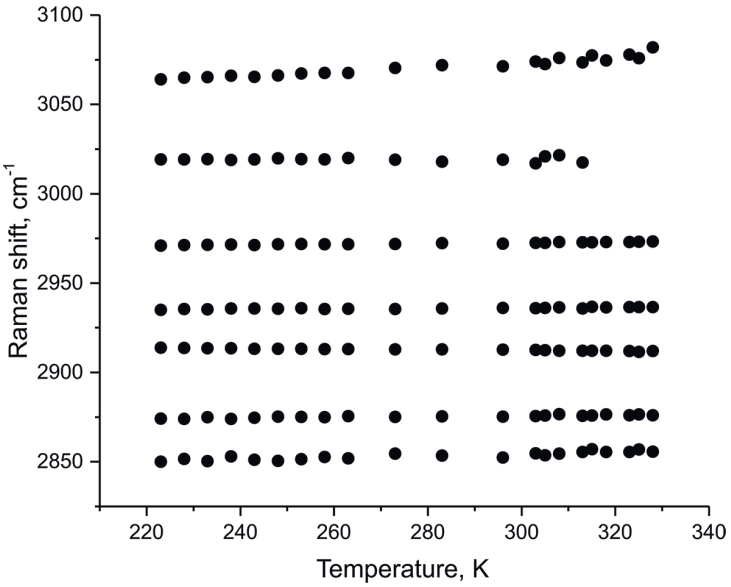

Fig. 3. Dependence of the Raman shifts of AgNPs on temperature in the range of 2780–3200 cm^{-1}

In the presence of a phase transition, the Raman spectrum undergoes changes, which are a jump in frequency, the appearance of new lines, and a non-chaotic change in intensity during further measurements. The spectral data were obtained from different points, which means a different orientation of the nanoparticles for each individual measurement; as a result, at different temperatures the intensity of individual lines is very different, but this does not indicate the presence or absence of a second-order phase transition in AgNPs.

A similar procedure for separating spectral contours into components was carried out for FeNPs (Fig. 4). Since iron is very actively oxidized when exposed to the atmosphere, double iron oxide $FeO\Delta Fe_2O_3$ (or Fe_3O_4) is formed on nanoparticles, and therefore it is very difficult to obtain vibrations of FeNP in its pure form.

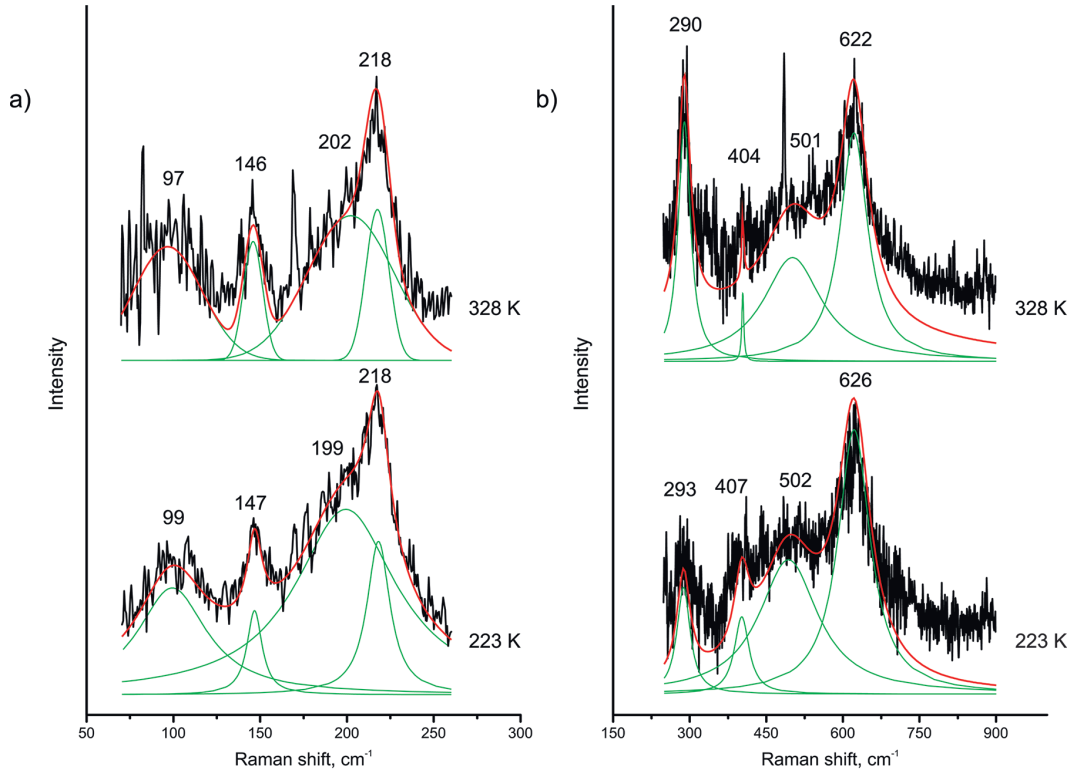

Fig. 4. Raman spectra of iron nanoparticles at different temperatures (indicated to the right of the spectrum) divided into different ranges: a) 60–260 cm^{-1}, b) 250–900 cm^{-1} (frequencies in cm^{-1} are indicated above the spectra)

Since iron atoms are much heavier than oxygen atoms, we can say that the more we descend into the low-frequency region, the more vibrations correspond to Fe atoms. The frequency range from 350 cm^{-1} and above refers to vibrations of O_2 molecules. The frequency range above 900 cm^{-1} is not considered due to the absence of spectral lines in it (Fig. 5).

Thus, vibrations at frequencies of 218 and 501 cm^{-1} belong to vibrations of the A_{1g} symmetry type. Vibrations occurring at frequencies of 146, 202, 290, 404 and 622 $cm^{-}1$ refer to vibrations of Eg symmetry type. Due to the high noise level compared to the intensity of the Raman spectrum in the region of about 100 cm^{-1}, it is not possible to resolve two separate lines at all temperatures, so the separation of the contour in this frequency range is not reliable. Within the specified temperature range, no significant deviations were found in the location of the spectral line maxima, which indicates the absence of phase transitions in silver and iron nanoparticles.

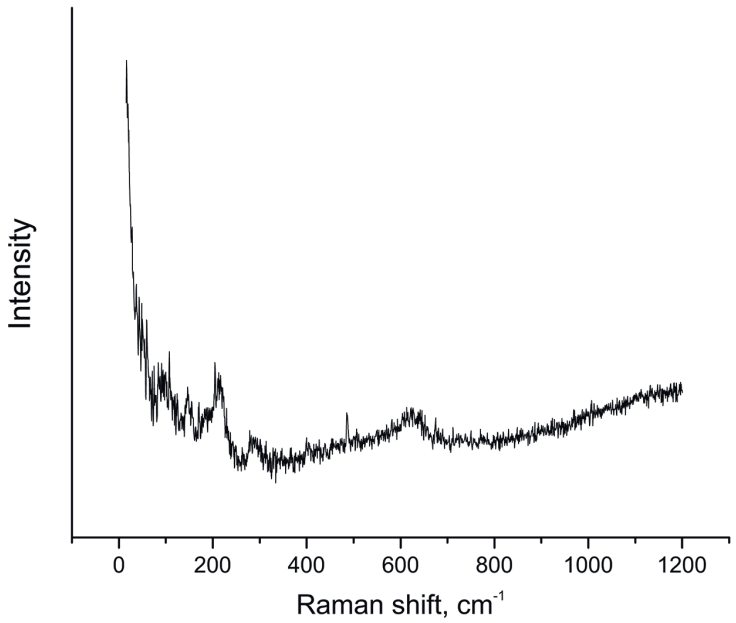

Fig. 5. Raman spectrum of AgNPs at room temperature

Also ultrasound attenuation spectra suspensions were collected. Fig. 6 shows the attenuation spectra of ultrasound in suspensions. The behavior of the ultrasound attenuation coefficients for suspensions with AgNPs and FeNPs is significantly different. For FeNPs suspensions, the attenuation coefficient grows with increasing radiation frequency, which indicates a predominantly viscous attenuation mechanism. For AgNPs suspensions, the behavior of the attenuation coefficient as a function of frequency is more complex. At frequencies below 30 MHz, the absorption coefficient decreases with increasing radiation frequency. With a further increase in frequency, the absorption coefficient grows. This behavior suggests that in this case, the predominant mechanism of sound attenuation is scattering by AgNPs.

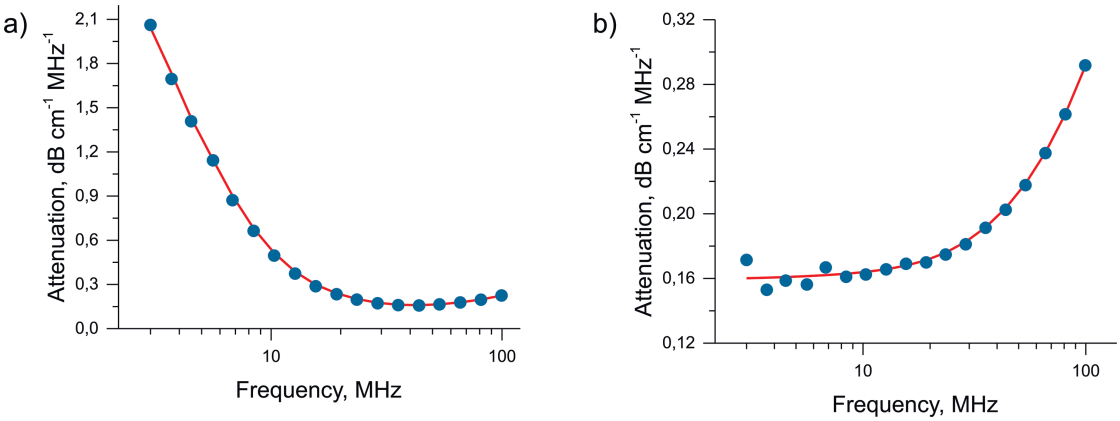

Fig. 6. Ultrasound attenuation spectrum in a 1% suspension: a) AgNPs; b) FeNPs

Based on the attenuation spectra, particle size distributions were obtained (Fig. 7). The average particle size in a silver suspension is 340 nm, and in an iron oxide suspension is 930 nm.

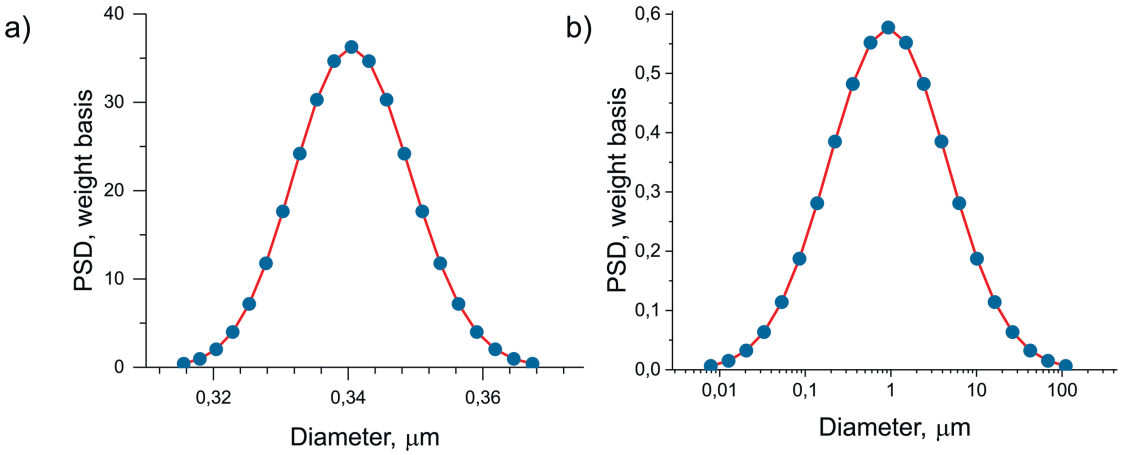

Fig. 7. Particle size distribution in water: a) AgNPs; b) FeNP

Conclusion

The Raman spectra of AgNPs and FeNPs were obtained in a wide frequency range within a temperature range from 223 K to 328 K. As a result of spectral data processing, the absence of abrupt changes in the spectral composition was shown, and the shifts of individual lines are linear, which indicates that the ongoing changes in the structure of the investigated particles remain within the limits of one phase. Also, it can be concluded that the particles have high structural stability, which makes them promising for use in the composition of colloidal suspensions with pronounced viscoelastic properties, which are used as lubricants for technological machines and equipment.

The mechanisms of attenuation on the studied nanoparticles were determined. Numerical values of the average sizes of silver and iron nanoparticles were also measured.

The authors would like to express their special thanks to Krasnoyarsk Regional Center of Research Equipment of Federal Research Center "Krasnoyarsk Science Center SB RAS" for providing measurements on Raman spectrometer Horiba Jobin Yvon T64000.

Experimental measurements of suspension attenuation of suspensions is partially financed by Ministry of Science and Higher Education of the Russian Federation (project no. FSRZ-2020-0012).

References

[1] R.C.Murdock, L.Braydich-Stolle, A.M.Schrand, J.J.Schlager, S.M.Hussain, Characterization of nanomaterial dispersion in solution prior to in vitro exposure using dynamic light scattering technique, *Toxicol. Sci.*, **101**(2008), 239–253. DOI: 10.1093/toxsci/kfm240

[2] S.Gurunathan, J.H.Park, J.W.Han, J.H.Kim, Comparative assessment of the apoptotic potential of silver nanoparticles synthesized by Bacillus tequilensis and Calocybe indica in MDA-MB-231 human breast cancer cells: Targeting p53 for anticancer therapy, *Int. J. Nanomed*, **10**(2015), 4203–4222. DOI:10.2147/IJN.S83953

[3] W.R.Li, X.B.Xie, Q.S.Shi, ZH.Y.eng, Y.S.Ou-Yang, Y.B.Chen, Antibacterial activity and mechanism of silver nanoparticles on Escherichia coli, *Appl. Microbiol. Biotechnol,* **85**(2010), 1115–1122. DOI: 10.1007/s00253-009-2159-5

[4] P.Mukherjee, A.Ahmad, D.Mandal, S.Senapati, et al., Fungus-mediated synthesis of silver nanoparticles and their immobilization in the mycelial matrix: A novel biological approach to nanoparticle synthesis, *Nano Lett.*, **1**(2001), 515–519. DOI: 10.1021/nl0155274

[5] S.Chernousova, M.Epple, Silver as antibacterial agent: Ion, nanoparticle, and metal, *Angew. Chem. Int. Ed.*, **52**(2013), 1636-1653.

[6] C.Y.Li, Y.J.Zhang, M.Wang, Y.Zhang, G.Chen, L.Li, D.Wu, Q.Wang, *Invivo* real-time visualization of tissue blood flow and angiogenesis using Ag_2S quantum dots in the NIR-II window, *Biomaterials*, **35**(2014), 393–400. DOI: 10.1016/j.biomaterials.2013.10.010

[7] I.Sondi, S B.alopek-Sondi, Silver nanoparticles as antimicrobial agent: A case study on E. coli as a model for Gram-negative bacteria, *J. Colloid Interface Sci.*, **275**(2004), 177–182. DOI: 10.1016/j.jcis.2004.02.012

[8] A.D.Breki, A.E.Gvozdev, The effect of oils with nanoparticles of solid lubricants on power loss in gears, *Izvestiya TulGU. Technical sciences*, **101**(2017), no. 4, 171–180 (in Russian).

[9] V.N.Matveenko, E.A.Kirsanov, S.V.Remizov, Rheology of structured disperse systems, *Moscow University Chemistry Bulletin*, **61**(2006), no. 6, 31–36.

[10] B.B.Badmaev, B.B.Damdinov, Investigation of shear-elasticity properties of organic liquids by acoustical method, *Acoustical Physics*, **47**(2001), no. 5, 561–563.

[11] V.N.Bakunin, G.N.Kuzmina, O.P.Parenago, Nanosized structures in hydrocarbon lubricants, *Rus. chem. J.*, **47**(2003), no. 2, 45–50 (in Russian).

[12] Manturova E.A., The use of nanomaterials and nanofunctional additives in promising technologies for lubricating the contact of the wheel flange with the side surface of the rail head, *Engineering journal of Don.*, (2010), no. 2, 139–148 (in Russian).

[13] N.Ya.Yahyaev, J.B.Begov, Batyrmurzaev Sh.D., Batyrmurzaev Sh.A., Lubricating composition for improving the tribological characteristics of a lubricant, *Friction, wear, lubrication*, (2010), no. 7, 29–32.

[14] D.S.Griersona, R.W.Carpock, Nanotribology of carbon-based materials, *Nanotoday*, **2**(2007), no. 5, 12-21. DOI: 10.1016/S1748-0132(07)70139-1

[15] T.Becker, F.Mugele, Nanofluidics: Molecularly thin lubricant layers under confinement, *Molecular Simulation*, **31**(2005), no. 6-7, 489–494. DOI: 10.1080/08927020412331337069

[16] T.Becker, F.Mugele, Mechanical properties of molecularly thin lubricant layers: experimental methods and procedures, *Journal of Physics: Condensed Matter*, **17**(2005), no. 9, 319–332. DOI: 10.1088/0953-8984/17/9/004

[17] Song, Q.X.Yang, F.Zhang, D.Zh.Su, Rheological Properties of Aircraft Grease Containing Nano-Additives, *Key Engineering Materials*, **419-420**(2009), 53–56. DOI:10.4028/www.scientific.net/KEM.419-420.53

[18] B.V.Ranishenka, G.Isic, P.Mojzes, S.N.Terekhov, A.Yu.Panarin, Surface modification of plasmonic nanostructures for SERS spectroscopy of biomolecules, 13th International Conference on the Interaction of Radiation with Solids, 2019, 485–488 (in Russian).

[19] I.R.Nabiev, R.G.Efremov, G.D.Chumanov, Surface-enhanced Raman scattering and its application to the study of biological molecules, *Physics-Uspekhi j.*, **31**(1988), 241–262.

[20] H.Mansour, H.Letifi, R.Bargougui, et al., Structural, optical, magnetic and electrical properties of hematite ($a - Fe_2O_3$) nanoparticles synthesized by two methods: polyol and precipitation, *J. Applied Physics A*, **123**(2017), no. 12, 787. DOI: 10.1007/s00339-017-1408-1

[21] J.C.M.Espinosa, R.C.Cerritos, et al., Characterization of Silver Nanoparticles Obtained by a Green Route and Their Evaluation in the Bacterium of Pseudomonas aeruginosa, *J. Crystals*, **10**(2020), no. 5, 395.

[22] T.Forestier, S.Mornet, N.Daro, et al., Nanoparticles of iron(ii) spin-crossover, *J. Chemical Communications*, (2008), no. 36, 4327–4329. DOI: 10.1039/b806347h

[23] Y.Wang, W.Ji, Z.Yu, R.Li, et al., Contribution of hydrogen bonding to charge-transfer induced surface-enhanced Raman scattering of an intermolecular system comprising p-aminothiophenol and benzoic acid, *J. The Royal Society of Chem.*, **16**(2014), no. 7, 3153–3161. DOI: 10.1039/c3cp54856b

[24] M.Pagliai, F.Muni–Miranda, V.Schettino, M M.uniz-Miranda, Competitive Solvation and Chemisorption in Silver Colloidal Suspensions, *Progr. Colloid Polym. Sci.*, **139**(2012), 39–44. DOI: 10.1007/978-3-642-28974-3_8

Устойчивость к температурному воздействию наночастиц серебра и железа

Баир Б. Дамдинов
Сибирский федеральный университет
Красноярск, Российская Федерация
Институт физического материаловедения СО РАН
Улан-Удэ, Российская Федерация
Александр А. Ершов
Чингис М. Митыпов
Сибирский федеральный университет
Красноярск, Российская Федерация
Ольга А. Максимова
Сибирский федеральный университет
Красноярск, Российская Федерация
Институт физики им. Л. В. Киренского СО РАН
Красноярск, Российская Федерация
Галина Н. Харук
Сибирский федеральный университет
Красноярск, Российская Федерация

Аннотация. В работе было проведено исследование наночастиц железа и серебра методом спектроскопии комбинационного рассеяния света. Спектры были получены при изменении температуры. Были получены значения частот отдельных спектральных линий для определения наличия или отсутствия фазовых переходов второго рода. На основании данных о смещении спектральных линий также можно сделать вывод об устойчивости объектов исследования при изменении внешних условий и о том, как это повлияет на изменения суспензий, в состав которых они входят.

Ключевые слова: суспензии наночастиц железа и серебра, смазочные материалы, комбинационное рассеяние света, смещение спектральных линий.